

Probing the *Borrelia burgdorferi* Surface Lipoprotein Secretion Pathway Using a Conditionally Folding Protein Domain[∇]

Shiyong Chen and Wolfram R. Zückert*

Department of Microbiology, Molecular Genetics, and Immunology, University of Kansas Medical Center,
3901 Rainbow Boulevard, Kansas City, Kansas 66160

Received 19 August 2011/Accepted 20 September 2011

Surface lipoproteins of *Borrelia* spirochetes are important virulence determinants in the transmission and pathogenesis of Lyme disease and relapsing fever. To further define the conformational secretion requirements and to identify potential lipoprotein translocation intermediates associated with the bacterial outer membrane (OM), we generated constructs in which *Borrelia burgdorferi* outer surface lipoprotein A (OspA) was fused to calmodulin (CaM), a conserved eukaryotic protein undergoing calcium-dependent folding. Protein localization assays showed that constructs in which CaM was fused to full-length wild-type (wt) OspA or to an intact OspA N-terminal “tether” peptide retained their competence for OM translocation even in the presence of calcium. In contrast, constructs in which CaM was fused to truncated or mutant OspA N-terminal tether peptides were targeted to the periplasmic leaflet of the OM in the presence of calcium but could be flipped to the bacterial surface upon calcium chelation. This indicated that in the absence of an intact tether peptide, unfolding of the CaM moiety was required in order to facilitate OM traversal. Together, these data further support a periplasmic tether peptide-mediated mechanism to prevent premature folding of *B. burgdorferi* surface lipoproteins. The specific shift in the OM topology of sequence-identical lipopeptides due to a single-variable change in environmental conditions also indicates that surface-bound *Borrelia* lipoproteins can localize transiently to the periplasmic leaflet of the OM.

Bacterial lipoproteins are a class of peripherally membrane associated proteins that play significant roles in various cellular and pathogenic processes (29). They are particularly important protagonists in the development of two arthropod-borne infectious diseases, Lyme borreliosis and relapsing fever. Abundantly displayed on the surfaces of the causative *Borrelia* spirochetes, they consequently dominate the spirochetes' interface with both the vector and the host. It is therefore not entirely surprising that a multitude of *Borrelia* lipoproteins have been shown to contribute significantly to transmission, infection, persistence, and disease (4, 7, 10, 31, 41).

Due to the required crossing of the outer membrane (OM), the sorting of major lipoproteins is inherently more complex in *Borrelia* than in other diderm bacteria. In the Gram-negative model organism *Escherichia coli*, the major lipoprotein Lpp has a known periplasmic function in tethering the OM to the peptidoglycan cell wall (11) but can also assume a transmembrane, partially surface exposed topology in its unbound form (19). In previous studies with two functionally and structurally divergent outer surface lipoproteins, *Borrelia burgdorferi* OspA and OspC, as well as the OspC-related protein *Borrelia turicatae* Vsp1, we showed that surface lipoprotein secretion pathways are likely distinct from those in proteobacteria but conserved within the genus (62). We found that established eubacterial lipoprotein-sorting rules governed by N-terminal residues proximal to the triacyl-modified cysteine did not apply

(22, 37, 40, 52, 53, 58). Yet lipoprotein-targeting instructions remained restricted to disordered N-terminal peptides that function as “tethers,” i.e., that link the folded domains of the protein to the triacyl membrane anchor (32, 33, 50, 51) (Fig. 1). Our previous data also suggested that OspA, OspC, and Vsp1 lipoprotein tether mutants that were blocked from translocation through the spirochetal OM folded prematurely within the periplasm (50). It remained unclear, however, whether the identified lipoprotein tether mutants localizing to the periplasmic leaflet of the OM represented the products of an aborted translocation event or were equivalent to translocation intermediates. Therefore, we set out to develop an experimental system that would allow us to “catch and release” borrelial lipopeptides on their way to the bacterial surface. Here we present data obtained with constructs in which *B. burgdorferi* surface lipoproteins are fused to calmodulin (CaM), a eukaryotic protein that undergoes reversible calcium-dependent folding (30, 59). Using a reformulated cation-controlled *Borrelia* growth medium and radiolabeling experiments, we show that calcium chelation-induced unfolding of CaM specifically permits the translocation of mutant OspA tether-CaM fusion proteins from the periplasmic leaflet of the OM to the bacterial surface. The requirement for chelation-mediated unfolding of these model lipoproteins can be bypassed by providing a wild-type (wt) OspA tether peptide in *cis*.

MATERIALS AND METHODS

Bacterial strains and growth conditions. *E. coli* strains TOP10 (Invitrogen) and XL10-Gold (Stratagene) were used for recombinant plasmid construction and propagation and were grown in Luria Bertani (LB) broth or on LB agar (Difco). *Borrelia burgdorferi* B31-e2 or B313, both of which are clones of type strain B31 (ATCC 35210), was used for recombinant expression of OspA-CaM fusion proteins (Table 1). B31-e2 (2) expresses endogenous OspA, while B313

* Corresponding author. Mailing address: Department of Microbiology, Molecular Genetics, and Immunology, University of Kansas Medical Center, 3901 Rainbow Boulevard, Kansas City, KS 66160. Phone: (913) 588-7061. Fax: (913) 588-7295. E-mail: wzueckert@kumc.edu.

[∇] Published ahead of print on 30 September 2011.

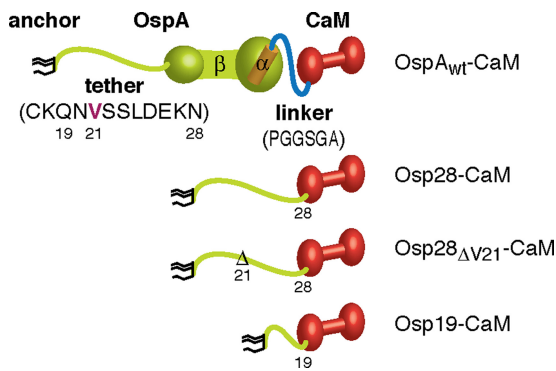


FIG. 1. OspA-CaM fusion constructs. Cartoons of OspA-CaM fusion constructs generated and used in this study show triacyl anchor lipids in black, OspA peptides in green (N-terminal tether and β-strands) and orange (C-terminal α-helix), linker peptides in blue, and CaM peptides in red. Tether and linker peptide sequences are given in one-letter amino acid code. Mutant nomenclature follows that of earlier publications (50, 51). Briefly, modified residues are numbered according to their lipoprotein positions; numbers in lipoprotein tether-CaM fusion constructs indicate the C-terminal tether residue present in the fusion.

lacks the lp54 plasmid encoding *ospA* (46, 62, 63). *B. burgdorferi* was cultured either in BSK-II medium (3, 60) or in BSK-SFcc, a cation-controlled modification of a BSK-II-based serum-free medium (18, 42). BSK-SFcc consisted of basal BSK-II medium (60) supplemented with 26 μM cholesterol, 12 μM palmitic acid, 12 μM oleic acid, 1 mM MgSO₄, 0.1 mM MnCl₂, and 0.1 mM ZnCl₂ (all from Sigma-Aldrich); divalent cations, including Ca²⁺, were chelated by two treatments with 2.5% (wt/vol) Chelex 100 (Sigma-Aldrich) before the Mn, Mg, and Zn ions, essential for the growth of *B. burgdorferi* (42), were added. Expression from the regulatable P_{ost} promoter (57) was induced by the addition of anhydrotetracycline hydrochloride (ATc; IBA GmbH, Göttingen, Germany) to the culture medium at a final concentration of 1 μg/ml. CaCl₂ and 1,2-bis(*o*-aminophenoxy)ethane-*N,N,N',N'*-tetraacetic acid (BAPTA) were used at standard final concentrations of 1 mM and 5 mM, respectively, unless otherwise noted.

OspA-CaM fusion proteins and point mutants. All plasmids generated and used in this study are derivatives of pBSV2 (56). The expression of OspA-CaM fusion proteins was driven either by the constitutive *B. burgdorferi* flagellin (*flaB*) promoter (P_{flaB}) or by the TetR-regulated hybrid P_{ost} promoter (57). Gene fusion constructs were generated by sequence overlap extension PCR (SOE-

PCR) (26) using Phusion (New England BioLabs/Finnzymes) high-fidelity DNA polymerase. Mutations were introduced using the QuikChange-II XL site-directed mutagenesis kit (Stratagene). Plasmids and custom oligonucleotides (Integrated DNA Technologies [IDT] DNA) are listed in Tables 1 and 2, respectively.

OspA_{wt}-CaM, a construct in which full-length wt OspA is fused to CaM via a 6-amino-acid linker peptide (Fig. 1), is encoded by pSC2001. The *ospA* gene was amplified from pSC0999 (50) using primer pair BamPflaB-fwd and OspA-Xcam-rev. The *Xenopus laevis* calmodulin gene (*cam*) lacking the *N*-formylmethionine codon was amplified from pBSXcam (a gift from Gerald Carlson, University of Kansas Medical Center) using the primer pair OspA-Xcam-fwd and Sph-Xcam-rev. The overlapping *ospA* and *cam* amplicons were fused using the flanking primer pair BamPflaB-fwd and Sph-Xcam-rev. In OspA28-CaM (Fig. 1) (pSC2002), CaM is fused to the 12-amino-acid OspA tether (51). Fragments containing the *ospA* tether peptide sequence, amplified from pRJS1009 (51) with BamPflaB-fwd and OspA28-Xcam-rev, and *cam*, amplified from pBSXcam with OspA28-Xcam-fwd and Sph-Xcam-rev, were fused by use of BamPflaB-fwd and Sph-Xcam-rev. The amplicons were then digested with BamHI and SphI and were ligated with an identically cut pRJS1009 backbone.

Constructs in which CaM was fused to the truncated OspA tether peptide OspA19 or OspA28_{ΔV21} (50, 51) were put under P_{ost} control. First, pCRW53 (57) was modified as follows. An NdeI site was introduced into the *gfp* gene start codon, and one NdeI site in the *kanR* gene cassette and two NdeI sites in the *tetR* gene cassette were removed, yielding pCRW56. The 3' end of the OspA tether sequence was removed from pSC2002 using OspA19-Xcam-fwd and OspA19-Xcam-rev in a QuikChange reaction, resulting in pSC2003, encoding OspA19-CaM (Fig. 1). The OspA Val²¹ codon was deleted from pSC2002 with primers OspA28-ΔV21-CaM-fwd and OspA28-ΔV21-CaM-rev, resulting in pSC2004, encoding OspA28_{ΔV21}-CaM (Fig. 1). PCR amplicons obtained with PflaBNdeospA-fwd and Xcam-XmaI-rev on pSC2003 and pSC2004 templates were digested with NdeI and XmaI and were ligated with an NdeI-BspEI-cut pCRW56 backbone, generating pSC2005 (OspA19-CaM) and pSC2006 (OspA28_{ΔV21}-CaM), respectively. All plasmids were verified by DNA sequencing (Center for Genetic Medicine, Genomics Core Facility, Northwestern University Medical Center, Chicago, IL, and ACGT, Wheeling, IL).

B. burgdorferi cells were transformed with 5 to 40 μg of plasmid DNA by electroporation using established protocols (47, 56). Transformants were selected in solid BSK-II medium containing 200 μg/ml kanamycin, and three independent clones were expanded in selective liquid BSK-II (60). Plasmid profiles were determined by PCR using plasmid-specific oligonucleotide primers (34, 44).

Gel electrophoresis and immunoblot analysis. Proteins were separated by sodium dodecyl sulfate-12% polyacrylamide gel electrophoresis (SDS-PAGE) and were visualized by Coomassie blue staining. For immunoblotting, proteins were electrophoretically transferred to an Immobilon-NC nitrocellulose membrane (Millipore) using a Transblot semidry transfer cell (Bio-Rad) as described

TABLE 1. Bacterial strains and plasmids used in this study

Strain or plasmid	Description	Source or reference
<i>Borrelia burgdorferi</i> strains		
B313	Clone of B31 ATCC 35210 (cp26, cp32-1, cp32-2/7, cp32-3, lp17); OspA ⁻	46
B31-e2	Clone of B31 ATCC 35210 (cp26, cp32-1, cp32-3, cp32-4, lp17, lp38, lp54); OspA ⁺	2
Plasmids		
pBSXcam	pBS vector containing the <i>Xenopus laevis cam</i> coding sequence (NCBI BC072232)	Gift from G. Carlson
pCRW53	pBSVΦ(<i>ospAp-gfp</i>) derivative with <i>gfp</i> gene under P _{ost} promoter control	14, 57
pCRW56	pCRW53 lacking Kan ^r cassette NdeI site and two Tet ^r cassette NdeI sites, with NdeI site introduced 5' of <i>gfp</i> gene	This study
pRJS1009	pBSV2::PflaBOspA28-mRFP1	51
pRJS1014	pBSV2::PflaBOspA19-mRFP1	51
pRJS1089	pBSV2::PflaBOspA28ΔV21-mRFPΔ4	50
pSC0999	pBSV2::PflaBospA-His, lacking pBSV2 BamHI/XmaI MCS ^a	50
pSC2001	pBSV2::PflaBOspA-CaM	This study
pSC2002	pBSV2::PflaBOspA28-CaM	This study
pSC2003	pBSV2::PflaBOspA19-CaM	This study
pSC2004	pBSV2::PflaBOspA28ΔV21-CaM	This study
pSC2005	pCRW56::Post OspA19-Xcam	This study
pSC2006	pCRW56::Post OspA28-ΔV21-CaM	This study

^a MCS, multiple-cloning site.

TABLE 2. Oligonucleotides used in this study

Name	Sequence (5' to 3')	Description
PflaBNdeospA-fwd	CATGGAGGAATGACATATGAAAAATATTTATTGGGAATAG	<i>ospA</i> gene cloning forward primer
KpnPflaB-fwd	CGGTACCCTGTCTGTCGCCTCTTG	<i>ospA</i> gene cloning forward primer
OspA-Xcam-fwd	AAACCGGGTGGCTCAGGTGCTGCTGACCAACTGACAGAAGAGC AGATTG	OspA-CaM fusion gene cloning forward primer
OspA-Xcam-rev	CTCTTCTGTCAGTTGGTCAGCAGCACCTGAGCCACCCGGTTTAA AAGCG	OspA-CaM fusion gene cloning reverse primer
BamPflaB-fwd	CGGGATCCTGTCTGTCGCCTCTTG	<i>flaB</i> promoter cloning forward primer
Sph-Xcam-rev	AAGCTTGCATGCTCATCACTTTGCTGTCATCATTTGTACAAACTC	SphI site introduction reverse mutagenic primer
OspA28-Xcam-rev	CTGCTCTTCTGTCAGTTGGTCAGCGTTTTTCTCGTCAAGGCTGC TAAC	OspA tether-CaM fusion cloning reverse primer
OspA28-Xcam-fwd	GTTAGCAGCCTTGACGAGAAAAACGCTGACCAACTGACAGAAG AGCAG	OspA tether-CaM fusion cloning forward primer
OspA19-Xcam-fwd	ATATTAGCCTTAATAGCATGTAAGCAAGCTGACCAACTGACAG AAGAGCAGA TTGCAGAG	OspA tether truncation (to aa 19) forward primer
OspA19-Xcam-rev	AATCTGCTCTTCTGTCAGTTGGTCAGCTTGCTTACATGCTATTAA GGCTAATATTAGACC	OspA tether truncation (to aa 19) mutagenic primer
OspA28-ΔV21-CaM-fwd	TTAATAGCATGTAAGCAAATAGCAGCCTTGACGAGAAAAACG CTGACCAACTG	V21 codon deletion forward mutagenic primer
OspA28-ΔV21-CaM-rev	AGTTGGTCAGCGTTTTTCTCGTCAAGGCTGCTATTTTGCTTACAT GCTATTAAGG	V21 codon deletion reverse mutagenic primer
Xcam-XmaI-rev	ATCAGCCCGGGTCACTTTGCTGTCATCATTTGTACAAACTC	XmaI site introduction reverse mutagenic primer

previously (62). Membranes were blocked and incubated with antibodies in 5% dry milk, 20 mM Tris–500 mM NaCl, and 0.05% Tween 20. The antibodies used were a rabbit polyclonal antiserum against monomeric red fluorescent protein 1 (mRFP1) (dilution, 1:1,000) (16), a rabbit polyclonal antiserum against OppAIV (dilution, 1:100) (8), or mouse monoclonal antibodies (MAbs) against Lp7.5/6.6 (MAb240.7) (dilution, 1:500) (28), OspA (H5332) (dilution, 1:100) (6), OspC (dilution, 1:50) (38), and FlaB (H9724) (dilution, 1:25) (5). CaM was detected by a rabbit monoclonal antibody (EP799Y; dilution, 1:1,500; Abcam). Secondary antibodies were alkaline phosphatase-conjugated goat-anti-rabbit IgG(H+L) or goat-anti-mouse IgG(H+L) (Sigma). Alkaline phosphatase substrates were 1-Step nitroblue tetrazolium (NBT)–5-bromo-4-chloro-3-indolylphosphate (BCIP) (Pierce) for colorimetric detection and CDP-Star (Amersham Biosciences) for chemiluminescent detection.

Protease and antibody accessibility assays. To assess the surface exposure of a protein by its accessibility to proteinase K, intact *B. burgdorferi* cells were harvested, washed, and treated *in situ* with 200 μg/ml proteinase K (Invitrogen) as described previously (12). Whole-cell protein preparations were analyzed by SDS-PAGE and Western immunoblotting.

Accessibility to antibodies was assessed by indirect fluorescent antibody assay (IFA) microscopy as described previously (63). Spirochetes were resuspended in phosphate-buffered saline (PBS) containing 5 mM MgCl₂ (PBS+Mg), 2% bovine serum albumin (BSA), with or without 0.06% (vol/vol) Triton X-100 (20), and were incubated with the primary antibodies described above against CaM (dilution, 1:300) or OppAIV (1:100). Fluorescein isothiocyanate (FITC)-labeled goat anti-rabbit IgG (whole molecule; dilution, 1:30; Sigma-Aldrich) was used as a secondary antibody. Cells were analyzed by epifluorescence microscopy using a Nikon Eclipse E600 microscope fitted with an FITC HYQ filter block. Digital images were acquired with a QImaging MicroPublisher digital charge-coupled device (CCD) color camera (epifluorescence micrographs), an Epson Perfection 2450 photo scanner, or a Fuji LAS-4000 luminescent image analyzer (immunoblots) and were processed using Adobe Photoshop CS4 for Macintosh.

Subcellular protein fractionation. Unless otherwise noted, *B. burgdorferi* membrane fractions were obtained using a hypotonic citrate buffer as described previously (51, 54). Briefly, *B. burgdorferi* cells were washed in 1× PBS containing 0.1% BSA, resuspended, and incubated under vigorous shaking for 2 h in 25 mM citrate buffer, pH 3.2, containing 0.1% BSA. Outer membrane vesicle (OMV) and protoplasmic cylinder (PC) fractions were separated by ultracentrifugation in a single discontinuous sucrose gradient in citrate buffer, washed, and resuspended in 1× PBS containing 1 mM phenylmethylsulfonyl fluoride (PMSF). An alternative, Ca²⁺ chelator-free (i.e., citrate-free) membrane fractionation approach was modified from reference 45 and used hypotonic sucrose buffer. Briefly, harvested *B. burgdorferi* cells were suspended in 20% (wt/vol) sucrose in 10 mM HEPES buffer, 150 mM NaCl, and 1 mM MgCl₂ (pH 7.4). After a 1-h

incubation, PC and OMV fractions were obtained by ultracentrifugation of the samples in an equal-volume stepped gradient of 20, 25, 30, 35, 40, 45, 50, 55, and 60% sucrose in a buffer consisting of 10 mM HEPES, 150 mM NaCl, and 1 mM MgCl₂ (pH 7.4). Fractions were washed and resuspended in HEPES buffer containing 1 mM PMSF. Both approaches used a Beckman L8-80M centrifuge with an SW28 rotor and 25- by 89-mm Ultra-Clear ultracentrifuge tubes.

Soluble and membrane-associated *B. burgdorferi* proteins were fractionated by Triton X-114 phase partitioning using a protocol modified from the work of Brandt et al. (10) and Nally et al. (39). Briefly, harvested cells were resuspended in a mixture of cold PBS and Mg (PBS+Mg) containing 2% (vol/vol) Triton X-114 (PBS+Mg+TX) and were incubated with end-over-end mixing at 4°C for 1 h. Samples were then heated to 37°C for 15 min and were centrifuged at room temperature for 15 min at 15,000 rpm. The detergent phase and the aqueous phase were separated into different tubes and were washed three times with 1 ml PBS+Mg or PBS+Mg+TX, respectively. Proteins in the detergent and aqueous phases were precipitated overnight in 4 sample volumes of acetone or 15% (vol/vol) trichloroacetic acid (TCA; Sigma), respectively, pelleted by centrifugation at 13,000 rpm for 15 min, washed with ice-cold acetone, and subjected to SDS-PAGE and Western blot analysis.

IP. Proteins were isolated from whole-cell lysates by immunoprecipitation (IP) using protein-specific antibodies and protein A Sepharose 4 Fast Flow beads (Amersham Biosciences) as described previously (51). Briefly, 5 × 10⁹ spirochetes were harvested and washed twice in ice-cold PBS+Mg. Cells were resuspended in 1 ml of ice-cold lysis buffer (50 mM Tris [pH 7.4], 1% dodecyl-β-D-maltoside [DDM], 1 mM PMSF) and were lysed using a Branson Sonifier cell disruptor. Cellular debris was pelleted by centrifugation for 10 min at 15,000 × g and 4°C. After preclearing with protein A beads for 1 h at 4°C, the lysate was incubated with an anti-Ca²⁺-CaM (ACC-1; dilution, 1:250; Millipore) (25) or an anti-CaM (EP799Y; dilution, 1:50; Abcam) antibody for 1 h at 4°C with end-over-end mixing. Next, 50 μl of washed protein A beads was added, and the incubation was continued for 1 h, after which the beads were washed three times with lysis buffer and once with 50 mM Tris, pH 7.4. Immunoprecipitated proteins were released from the beads by boiling for 5 min in 40 μl of SDS-PAGE sample buffer, collected in 30 μl of supernatant, and analyzed by SDS-PAGE and immunoblotting with an anti-CaM antibody.

Hydrophobic interaction chromatography (HIC). A total of 2.5 × 10⁹ late-log-phase spirochetes were harvested, washed three times with PBS+Mg, resuspended in 1.5 ml lysis buffer (50 mM Tris [pH 7.4], 1 M NaCl, 1% DDM, 1 mM PMSF), and lysed by sonication. The lysate was cleared by centrifugation for 10 min at 15,000 × g and 4°C. A 50-μl volume of phenyl-Sepharose CL-4B (Pharmacia LKB Biotechnology) preequilibrated in lysis buffer was added, and the mixture was mixed end-over-end for 2 h at 4°C. Subsequently, the supernatant was removed, and the resin was washed three times with lysis buffer without 1%

DDM and once with wash buffer (50 mM Tris-HCl buffer [pH 7.4], 1 mM PMSF). Proteins were eluted by incubating the resin in 0.6 ml wash buffer containing 1 mM EGTA for 10 min at 4°C with end-over-end rotation. The eluted proteins were concentrated by precipitation with TCA and were analyzed by SDS-PAGE and Western immunoblotting with the anti-CaM antibody.

Protein radiolabeling. A total of 5×10^8 early-log-phase spirochetes were harvested, washed once with PBS+Mg, and resuspended in 0.5 ml protein-free RPMI 1640 medium (pH 7.5; Sigma-Aldrich) containing a cysteine- and methionine-free amino acid mixture and appropriate antibiotics. Final concentrations of 1 $\mu\text{g/ml}$ ATc and 100 $\mu\text{Ci/ml}$ [^{35}S]Cys-Met (EasyTag Express ^{35}S protein labeling mix; Perkin-Elmer) were added to simultaneously induce P_{ost} promoter-driven expression of OspA-CaM fusion proteins and metabolic radiolabeling of cellular proteins. After incubation for 2 h at 34°C, the cells were pelleted, resuspended in RPMI 1640 medium containing 1.5 mg/ml cold Cys and Met, and incubated for 10 min at 34°C. The spirochetes were then pelleted and resuspended in BSK-SFcc medium containing either calcium or BAPTA (final concentrations, 5 mM). After incubation for 3 h at 34°C, the cells were harvested, washed twice with PBS+Mg, and subjected to *in situ* proteolysis. SDS-PAGE gels containing whole-cell proteins were stained with 0.05% Coomassie brilliant blue R-250 (Sigma) in 40% methanol and 10% acetic acid, destained with 20% methanol and 10% acetic acid, and immersed in Amplify fluorographic reagent (Amersham Biosciences) for 30 min. After drying under a vacuum for 1 h at 60°C, the gels were exposed overnight to Kodak (Rochester, NY) XAR-5 film.

RESULTS

Development of OspA-CaM fusion proteins and a cation-controlled *Borrelia* culture medium. CaM undergoes a significant conformational change upon the binding of calcium cations (Ca^{2+}). The Ca^{2+} -free apo-form is largely unfolded, whereas the Ca^{2+} -loaded protein forms a stable dumbbell structure (30). Hence, the folding state of CaM can be controlled by experimentally manipulating the Ca^{2+} level (1, 24, 27, 59). To test whether the addition of a tightly folded Ca^{2+} -CaM domain could block the secretion of a *Borrelia* surface lipoprotein, we generated OspA-CaM fusion proteins (Fig. 1). Because the standard BSK-II medium contains rich sources of calcium, such as rabbit serum, we modified a serum-free *Borrelia* “minimal medium” developed by Posey and Gherardini (42) and by Cluss et al. (18) to allow for more-precise control of Ca^{2+} levels. As expected, the growth characteristics of *B. burgdorferi* in the standard culture medium BSK-II and the calcium-free medium BSK-SFcc were comparable (Fig. 2). Mean log-phase generation times were 13.9 h in BSK-II medium and 16.9 h in BSK-SFcc. Addition of Mg, Mn, and Zn ions was sufficient to support growth in a previously chelated medium, as shown for the similarly formulated medium used by Posey and Gherardini (42). These preliminary experiments confirmed that calcium-limiting conditions had no significant effects on cell growth that would introduce additional undesired variables into the experimental setup.

Tolerance of the *B. burgdorferi* lipoprotein secretion machinery for wild-type OspA-CaM fusion constructs. The first constructs to be tested had CaM fused either to full-length wild-type OspA (OspA_{wt}-CaM) or to the OspA_{wt} tether peptide (OspA28-CaM) (Fig. 1; Table 1). *B. burgdorferi* transformants expressing the two fusion proteins were grown in the selective medium BSK-SFcc supplemented with either 1 mM calcium chloride or 5 mM BAPTA, a calcium-specific chelator. Based on accessibility to proteolytic shaving with proteinase K, both OspA_{wt}-CaM and OspA28-CaM fusion proteins were displayed on the bacterial surface, irrespective of the presence of calcium ions or the chelator (Fig. 3A). The folding statuses of the fusion proteins under both experimental conditions were

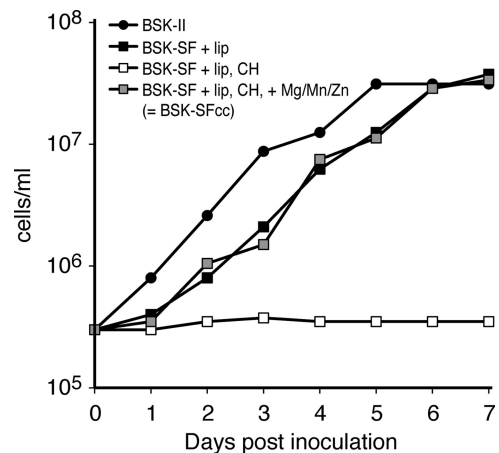


FIG. 2. Growth of *B. burgdorferi* in serum- and calcium-free minimal medium. *B. burgdorferi* was cultured in complete BSK-II medium and in various modifications of serum-free (SF) medium. Serum-free incomplete or basal BSK medium (BSK-SF) (60) was supplemented with lipids (+ lip), treated with Chelex-100 (CH), or supplemented with essential cations (+Mg/Mn/Zn). Cells were counted under phase-contrast microscopy using a Petroff-Hausser counting chamber. Representative growth curves are shown. Note that the 1-day lag phase for cells grown in BSK-SFcc persisted even when bacteria had been passed in BSK-SFcc previously (data not shown).

analyzed by two independent approaches: (i) IP with a Ca^{2+} -CaM fold-specific antibody (25) and (ii) HIC, which takes advantage of the specific hydrophobic interaction of the Ca^{2+} -bound CaM with phenyl Sepharose (23). The CaM contents of the samples obtained by IP and HIC were then assayed by Western immunoblotting with a fold-independent anti-CaM antibody. Figure 4 shows that the availability of Ca^{2+} in the culture medium clearly enriched for interaction of the CaM fusion proteins with both the Ca^{2+} -CaM-specific antibody and phenyl Sepharose, while the BAPTA chelator suppressed such enrichment. Together, these experiments demonstrated that the folding state of CaM within an OspA fusion construct could indeed be modulated by supplementation with, or chelation of, calcium ions. They also indicated that the *B. burgdorferi* lipoprotein secretion machinery properly secreted CaM-containing lipopeptides even in the presence of Ca^{2+} , provided that the fusion proteins contained at least a wild-type OspA tether.

Calcium chelation-dependent OM translocation of “periplasmic” OspA-CaM fusion proteins. We next fused CaM to the shortened OspA tether peptides OspA28 _{Δ V21} and OspA19. In previous studies, these tether peptides had targeted the monomeric red fluorescent protein (mRFP) reporter protein mRFP1 or its derivative mRFP Δ 4 to the periplasm (50, 51). *B. burgdorferi* transformants expressing the OspA28 _{Δ V21}-CaM or OspA19-CaM fusion protein were grown in the selective medium BSK-SFcc supplemented with either calcium chloride or BAPTA as described above. IP and HIC experiments, as described above for the OspA_{wt}-CaM and OspA28-CaM fusion proteins, confirmed that both the OspA28 _{Δ V21}-CaM and OspA19-CaM fusion proteins were able to undergo Ca^{2+} -dependent folding as well (Fig. 4).

Western immunoblotting of Triton X-114 detergent fractions showed that the OspA19-CaM and OspA28 _{Δ V21}-CaM

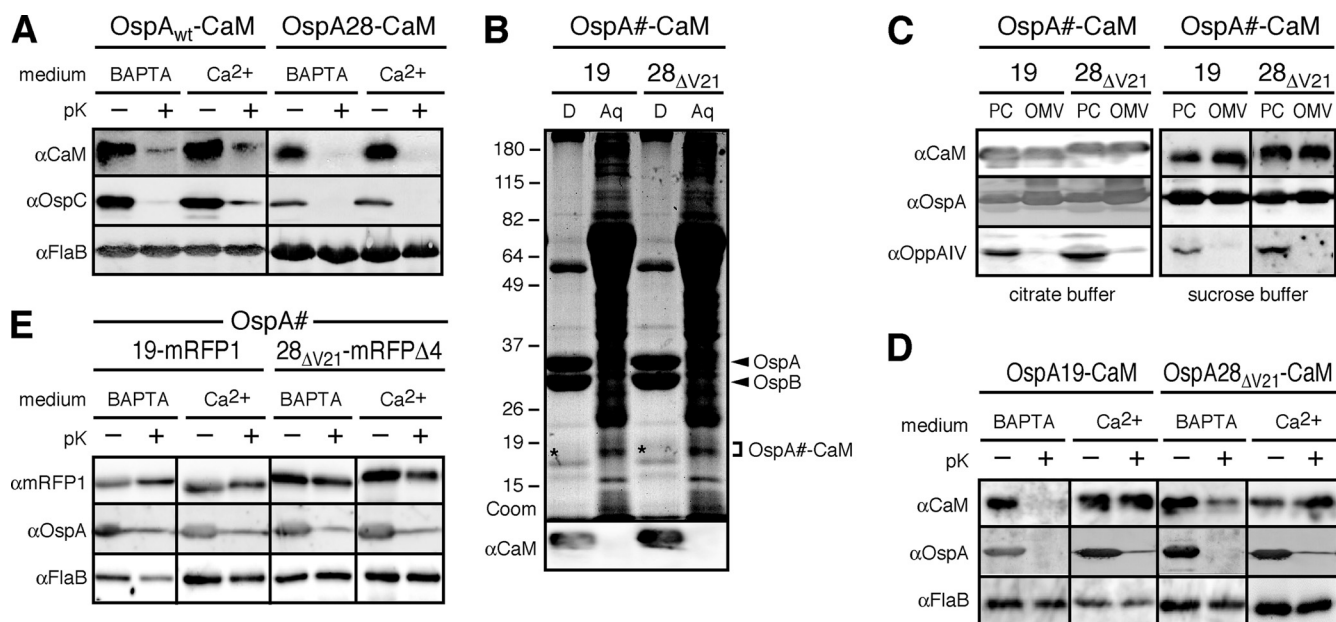


FIG. 3. Chelation-dependent surface exposure of OspA-CaM fusion proteins at steady state. (A) Accessibility of full-length OspA-CaM or OspA tether-CaM fusion proteins to proteinase K. Cells expressing the fusion constructs were grown in BSK-SFcc containing either Ca^{2+} or BAPTA. Lipoprotein surface exposure was assessed by incubating intact cells with proteinase K (pK+) or a control buffer (pK-), followed by Western immunoblotting with antibodies against CaM, OspC (used as an OspA-independent surface control, due to the coexpression of endogenous OspA_{wt} and OspA_{wt} -CaM), and FlaB (periplasmic control) (αCaM , αOspC , and αFlaB , respectively). (B) Total-protein fractionation by Triton X-114 of *B. burgdorferi* cells expressing the $\text{OspA}_{28\Delta\text{V}21}$ -CaM or OspA_{19} -CaM fusion protein in the presence of Ca^{2+} . A Coomassie-stained SDS-PAGE gel (Coom) and an immunoblot with αCaM are shown. D, detergent phase; Aq, aqueous phase. The positions of OspA and OspB are indicated on the right. Asterisks indicate the weakly Coomassie stained OspA-CaM fusion bands present in the respective detergent fractions. (C) Membrane fractionation immunoblots of the subsurface $\text{OspA}_{\Delta\text{V}21}$ -CaM and OspA_{19} -CaM fusion proteins expressed by *B. burgdorferi* in the presence of Ca^{2+} . OppAIV served as an inner membrane control, and OspA served as an OM control. PC, protoplasmic cylinder fraction; OMV, outer membrane vesicle fraction enriched for OM proteins. Note that the PC fraction also contains OM proteins, because OMVs were only partially separated from protoplasmic cylinders by treatment of *Borrelia* cells with a hypotonic citrate buffer; therefore, the PC fraction is similar to a whole-cell protein preparation (54). (D) Accessibility to proteinase K of partial or mutant OspA tether-CaM fusion proteins expressed by *B. burgdorferi*. The experimental procedures and labels described for panel A were used, except that OspA was used as the standard surface control. (E) Accessibility to proteinase K of previously described periplasmic OspA-mRFP fusion proteins (50, 51) under calcium-containing (Ca^{2+}) or chelating (BAPTA) conditions. The experimental procedures and labels were the same as those for panel D.

fusion proteins were associated with the membrane (Fig. 3B). Outer membrane vesicle (OMV) fractions obtained by treatment of cells cultured in BSK-II medium with a hypotonic citrate buffer (51, 54) showed that both CaM fusion proteins localized to the OM (Fig. 3C, left). Because citrate has Ca^{2+} -chelating activity, which might influence the folding and localization of the CaM fusion proteins during the procedure, we repeated the assay with an alternative membrane fractionation protocol using a chelator-free hypotonic sucrose buffer (45) (Fig. 3C, right). The two fractionation protocols yielded identical results. It should be noted that the "protoplasmic cylinder" (PC) fractions obtained by both protocols also contain OM proteins; this is due to the inefficient release of OMVs and therefore the presence of intact cells in the PC fraction (54). Therefore, the PC fractions presented here and elsewhere should be considered similar to whole-cell protein preparations.

In proteinase K accessibility assays, the presence of Ca^{2+} protected both $\text{OspA}_{28\Delta\text{V}21}$ -CaM and OspA_{19} -CaM fusion proteins from cleavage, while chelation with BAPTA rendered both fusion proteins accessible to proteolysis (Fig. 3D). In addition to the standard periplasmic FlaB control, we assayed the previously described constructs in which the identical

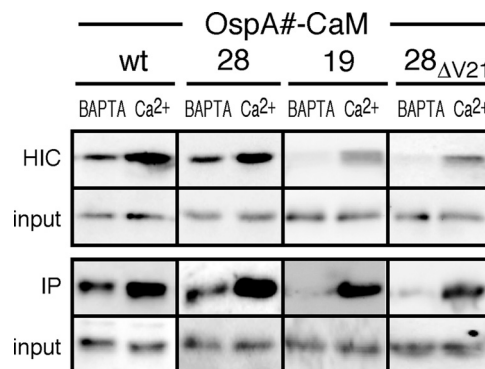


FIG. 4. Assessment of the folding states of the OspA-CaM fusion proteins by hydrophobic interaction chromatography (HIC) and immunoprecipitation (IP). Western blot analysis was performed on OspA-CaM fusion proteins purified by HIC or IP from whole-cell lysates of recombinant *B. burgdorferi* cultured in the presence of Ca^{2+} or BAPTA. Phenyl Sepharose was used to enrich for the folded CaM fusion proteins by HIC. For IP experiments, CaM fusion proteins were immunoprecipitated with a Ca^{2+} -CaM complex-specific monoclonal antibody. For both the HIC and IP approaches, equal ratios of whole-cell lysates (input) were loaded for comparison. OspA-CaM fusion proteins in both the input and eluted pulldown samples were detected by immunoblotting with a non-conformation-specific antibody against CaM.

OspA tether peptides were fused either to mRFP1 (OspA19-mRFP1) (51) or to its derivative mRFPΔ4 (OspA28_{ΔV21}-mRFPΔ4) (50). As shown previously for proteins harvested from cultures grown in standard BSK-II broth (47, 48), both OspA-mRFP fusion proteins remained localized to the periplasm under both Ca²⁺-containing and Ca²⁺-free conditions (Fig. 3E). These steady-state differences suggested that calcium chelation specifically stimulated the unfolding and translocation of lipopeptide-CaM fusion proteins through the borrelial OM.

Calcium chelation-induced rescue of translocationally blocked OspA-CaM fusion proteins. The dynamics of lipoprotein secretion in *B. burgdorferi* have not been determined precisely, but the time appears to be in the range of several hours (20). It therefore remained possible that the chelation-dependent steady-state surface localization of OspA28_{ΔV21}-CaM and OspA19-CaM proteins described above was due to the proper secretion of fusion proteins newly expressed under Ca²⁺-free conditions. In an attempt to exclude this possibility and to concurrently gain further insight into lipoprotein secretion kinetics, we used a radiolabeling approach in conjunction with our recently described tetracycline-responsive P_{ost} promoter system (57). This combination allowed us first to express and label cohorts of OspA19-CaM or OspA28_{ΔV21}-CaM molecules under conditions that blocked their translocation through the OM and then to observe the protein cohorts' fate when that restriction was lifted. Recombinant *B. burgdorferi* cells grown in Ca²⁺-containing BSK-SFcc were resuspended in RPMI 1640 medium, where recombinant lipoprotein expression and ³⁵S metabolic protein labeling were initiated concurrently for 2 h. After a 10-min incubation in RPMI 1640 medium with cold amino acids, cells were incubated in BSK-SFcc containing either Ca²⁺ or BAPTA for 2 h, harvested, and subjected to *in situ* proteolysis and fluorography analysis. As shown in the lower panel of Fig. 5, the 19- to 20-kDa bands corresponding to either OspA19-CaM or OspA_{ΔV21}-CaM appeared only upon induction of the P_{ost} promoter with ATc and remained protected from proteolysis in the presence of Ca²⁺. BAPTA treatment, however, rendered the CaM fusion proteins susceptible to *in situ* proteinase K treatment on the spirochetal surface. In agreement with the OspA-mRFP data shown in Fig. 3E, there were no discernible pleiotropic effects on other borrelial proteins. Western immunoblotting for the lipidated CaM proteins and the OspA and FlaB controls confirmed these findings (Fig. 5, upper panel).

In a complementary approach, we checked for release of periplasmically trapped CaM lipopeptides by immunofluorescence microscopy as described previously (51). To visualize total or subsurface proteins, cells were permeabilized with Triton X-100 prior to incubation with antibodies (20). Immunofluorescence due to the interaction of specific antibodies with the CaM fusion proteins was observed only in the presence of BAPTA or with detergent-permeabilized cells. At the same time, only detergent permeabilization, not BAPTA treatment, led to accessibility of the inner membrane lipoprotein OppAIV (8, 51; also data not shown). Together, these assays confirmed that Ca²⁺ chelation led to the specific and rapid release of lipopeptide-CaM fusion proteins from the periplasm to the *B. burgdorferi* surface.

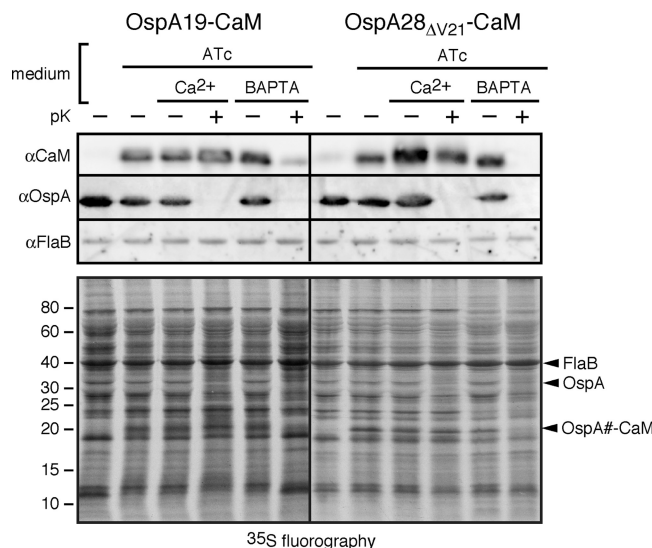


FIG. 5. Chelation-dependent surface exposure of radiolabeled, conditionally expressed OspA-CaM fusion proteins. (Top) Western immunoblot analysis; (bottom) fluorography analysis. Prior to analysis, *B. burgdorferi* cells were cultured to early-log phase in BSK-SFcc containing Ca²⁺. Radiolabeling with [³⁵S]Cys-Met amino acids and anhydrotetracycline (ATc)-mediated induction of P_{ost} promoter-driven expression were initiated simultaneously in RPMI 1640 medium. Subsequently, cells were incubated in BSK-SFcc containing either Ca²⁺ or BAPTA, followed by *in situ* surface proteolysis with proteinase K (+pK). Total fusion proteins expressed upon ATc induction were detected by Western immunoblotting with antibodies against CaM, OspA (surface control), and FlaB (subsurface control), while fluorography detected proteins expressed during the pulse. The proteins bands detected by Western immunoblotting are indicated on the right.

DISCUSSION

The deployment of bacterial virulence factors to their proper compartments is essential to microbial pathogenesis. For the surface lipoproteins involved in the colonization, persistence, and pathogenesis of *Borrelia* spirochetes, this involves the crossing of two lipid bilayers as well as the intervening aqueous periplasm. In this study, we focused on the molecular events at the OM by fusing N-terminal tether peptides of the *B. burgdorferi* surface lipoprotein OspA to the calcium-binding eukaryotic protein CaM. Thus, we were able to demonstrate that the same OspA-CaM fusion proteins that were restricted to the periplasmic leaflet of the OM under experimental conditions that favored folding regained their capacity to be translocated through the OM under experimental conditions that induced unfolding. These findings are in accordance with our earlier interpretations of individual sets of OspA and OspC lipoprotein mutant phenotypes, where periplasmic OspA and OspC tether mutants could be redirected to the bacterial surface by mutational destabilization of a C-terminal α -helix or by the addition of short disordered C-terminal epitope/affinity tags, respectively (32, 50). Interestingly, the present study reiterates that C-terminal structural destabilization, achieved this time by chelating Ca²⁺ from an admittedly larger calmodulin “tag,” is sufficient to promote secretion through the OM. Thus, the current findings corroborate the requirement for the delivery to the OM of a translocation-competent surface lipoprotein molecule that is at least partially unfolded. They also remain

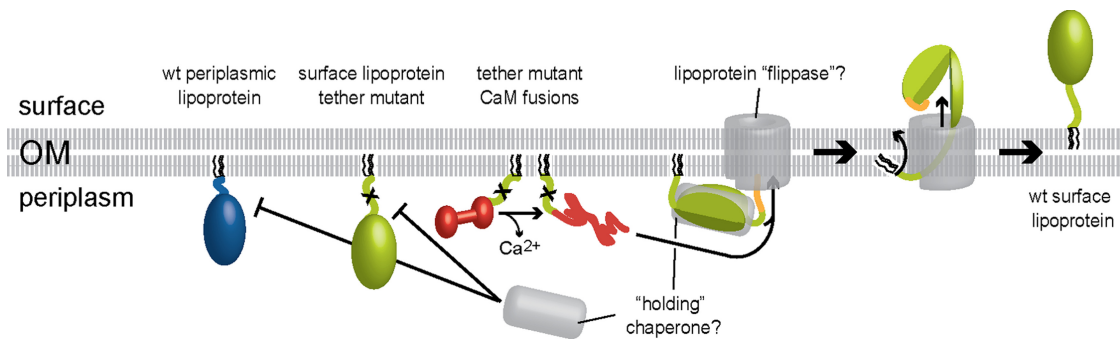


FIG. 6. Proposed molecular events at the *B. burgdorferi* OM during surface lipoprotein secretion. Where possible, the color scheme follows that of Fig. 1. Hypothetical components are drawn in gray. Tether mutants of surface lipoproteins such as OspA (light green, with an X marking the tether mutation) fold prematurely in the periplasm, and their secretion through the OM is thereby prevented (17, 18). Periplasmic folding or interactions with periplasmic envelope components may be responsible for subsurface retention of wt periplasmic lipoproteins such as Lp6.6 (blue). Translocation of periplasmic mutant OspA tether-CaM fusion proteins (red) is dependent on chelation-mediated structural changes (this study). Intact surface lipoprotein tether peptides prevent premature folding of proteins—and thereby allow for OM translocation—via interaction with a hypothetical “holding” chaperone (gray). As shown for wt OspA (but also valid for the wt OspA-CaM fusion protein), translocation can initiate at the lipoprotein’s C terminus if an unfolded peptide is provided (50; also this study). The peptide portion travels via the hydrophilic lumen of a hypothetical OM lipoprotein “flippase” pore (gray), while the lipid anchor (black) flips from the periplasmic leaflet to the surface leaflet of the OM bilayer; this ultimate anchor topology was recently shown for OspA and *B. turicatae* Vsp1 (17). In the absence of ATP, the directionality of the process is likely driven by the folding and assembly of the protein on the bacterial surface. This figure updates the *Borrelia* envelope biogenesis model shown in the work of Bergström and Zückert (7).

compatible with the potential C-to-N vectoriality of surface lipoprotein translocation proposed previously (50) (Fig. 6).

How wt borrelial surface lipoproteins are maintained in such a translocation-competent conformation remains to be revealed. Yet it is becoming increasingly clear that lipoprotein tether peptides play a central role in this process. As demonstrated here, the secretion requirement for chelation-mediated unfolding of CaM can be circumvented if an intact surface lipoprotein N terminus is provided *in cis*, either as part of a full-length OspA protein or by a full-length OspA28 tether peptide (Fig. 1 and 6). This finding again closely correlates with our earlier observations: wt tether peptides of OspA and OspC were able to properly direct mRFP reporter proteins to the spirochetel surface, whereas mutant tether peptides (mis)localizing OspA, OspC, and mRFP to the periplasm did not prevent protein folding and, in the case of mRFP, periplasmic activity, observed as red fluorescence (32, 50, 51). Our previous studies indicated the absence of any minimal tether length requirement for lipoprotein surface localization (50, 51). Also, an OspC tether peptide had no intrinsic structure-destabilizing properties (32). One interpretation that remains consistent with all currently available data is that surface lipoprotein tethers are involved indirectly in proper targeting by enabling interaction with a periplasmic “holding” chaperone that prevents its cargo from premature periplasmic folding (Fig. 6). If this were indeed the case, sequestration of surface lipoprotein tether mutants, and possibly wt periplasmic OM lipoproteins, such as Lp6.6 (43), to the periplasm could be explained by their failure to interact with this lipoprotein secretion pathway component (Fig. 6). Such a chaperone-mediated mechanism may be similar to the interaction of the pilin subunits of Gram-negative bacteria with their cognate periplasmic chaperones, which prevents untimely periplasmic pilus assembly and guides the complex to the OM assembly platform (the usher) (49). Yet in light of the tether peptide divergence among the numerous surface lipoproteins encoded by the *Borrelia* genome,

with only 1.6 Mbp (15, 21, 50), a likely single chaperone would have to be quite promiscuous in its interactions, i.e., it would have to function similarly to the Skp and/or SurA chaperones, which are involved in shepherding integral OM protein peptides through the periplasm (9, 55).

The data presented here also raise the potential for transient anchoring of surface *B. burgdorferi* surface lipoproteins within the periplasmic leaflet of the OM. One of our recent studies already hinted at that possibility, but our preliminary conclusions at the time were based on steady-state OM topologies of a combinatorial series of different OspA mutants under identical experimental conditions (50). Here, the use of a model lipoprotein system undergoing conditional conformational change allows us to substantiate these interpretations by identifying the topologies of identical lipopeptides under different environmental conditions. The apparent tolerance of the *B. burgdorferi* lipoprotein secretion machinery for CaM domains and the stability of the periplasmic OspA-CaM mutants is intriguing in the context of two findings for Gram-negative diderm bacteria. In one study, replacement of an internal passenger subdomain of the *E. coli* type V “autotransporter” secretion protein Hbp with CaM blocked secretion, leading to envelope stress and degradation of the fusion protein by the periplasmic protease DegP (27). A similar CaM-dependent secretory block was seen with *E. coli* intimin, an intimin/invasin-type protein (1). Based on the absence of a secretion block phenotype with the OspA_{wt}-CaM fusion proteins, one might therefore argue that the association of the mutant OspA-CaM fusion proteins with the periplasmic OM leaflet is “off-pathway.” Our current data cannot fully exclude such a conclusion. However, the differing effects of introducing a CaM moiety into the three experimental systems may be due simply to the significant variability in their structures and secretion mechanisms. Also, the surface phenotype of the wt OspA-CaM fusion protein could be explained by the prevention of folding via a tether-mediated association with a periplasmic protein, men-

tioned above. Most importantly, an “off-pathway” periplasmic surface lipoprotein mutant would be unlikely to retain its ability to be flipped to the surface, i.e., it would be incompatible with the conditional topologies of two separate OspA tether-CaM fusion proteins demonstrated here. We recently demonstrated that OspA and *Borrelia turicatae* Vsp1, a structural homolog of *B. burgdorferi* OspC (35, 61), are anchored in the surface leaflet of the spirochetal OM (17), i.e., they ultimately adopt an “outside anchor-outside protein,” or “out-out,” topology. This finding corroborated prior indirect evidence obtained with recombinant lipidated OspA and OspA-mRFP1 fusion proteins (13, 50, 51). The transbilayer crossing of the OM by borrelial surface lipoproteins may therefore be mechanistically similar to that of other lipidated bacterial cell envelope components. Grounded in the reductionist observations of polar lipid behavior in bilayers, several mechanistic models have been proposed; all involve “flipping” of the lipid moiety sequestered to the hydrophobic environment, while hydrophilic moieties are translocated through a protein channel such as a “flippase” or at least through interaction with a transmembrane protein (48) (Fig. 6). While the existence, identity, and role of a similar pathway component remain to be established, *B. burgdorferi* surface lipoprotein secretion appears to be at least indirectly dependent on a homolog of the OM β -barrel assembly machinery protein BamA (36).

Together, these findings encourage us to further elucidate the precise molecular mechanism of OM crossing by spirochetal surface lipoproteins. To that end, we are currently using our regulatable P_{ost} promoter system (57) to generate conditional knockouts of several pathway candidates. At the same time, we are also further deploying CaM as well as protein-protein interaction approaches to advance our understanding of the individual steps involved in the secretion of this important class of *Borrelia* virulence factors.

ACKNOWLEDGMENTS

This research was supported by the National Institutes of Health (grant R01 AI063261 to W.R.Z.).

We thank Christine Whetstone and Eszter Adany for experimental support, Frank Gherardini and Bob Cluss for advice on culture medium composition, and Gerald Carlson and Owen Nadeau for the recombinant calmodulin-encoding plasmid. We are also grateful to Joe Lutkenhaus, Ryan Schulze, and Brian Stevenson for inspiring discussions and helpful comments on the manuscript.

REFERENCES

- Adams, T. M., A. Wentzel, and H. Kolmar. 2005. Intimin-mediated export of passenger proteins requires maintenance of a translocation-competent conformation. *J. Bacteriol.* **187**:522–533.
- Babb, K., J. D. McAlister, J. C. Miller, and B. Stevenson. 2004. Molecular characterization of *Borrelia burgdorferi* *erp* promoter/operator elements. *J. Bacteriol.* **186**:2745–2756.
- Barbour, A. G. 1984. Isolation and cultivation of Lyme disease spirochetes. *Yale J. Biol. Med.* **57**:521–525.
- Barbour, A. G., and B. P. Guo. 2010. Pathogenesis of relapsing fever, p. 333–357. In D. S. Samuels and J. D. Radolf (ed.), *Borrelia: molecular biology, host interaction, and pathogenesis*. Caister Academic Press, Norfolk, United Kingdom.
- Barbour, A. G., S. F. Hayes, R. A. Heiland, M. E. Schrupf, and S. L. Tessier. 1986. A *Borrelia*-specific monoclonal antibody binds to a flagellar epitope. *Infect. Immun.* **52**:549–554.
- Barbour, A. G., S. L. Tessier, and W. J. Todd. 1983. Lyme disease spirochetes and ixodid tick spirochetes share a common surface antigenic determinant defined by a monoclonal antibody. *Infect. Immun.* **41**:795–804.
- Bergström, S., and W. R. Zückert. 2010. Structure, function and biogenesis of the *Borrelia* cell envelope, p. 139–166. In D. S. Samuels and J. D. Radolf (ed.), *Borrelia: molecular biology, host interaction, and pathogenesis*. Caister Academic Press, Norfolk, United Kingdom.
- Bono, J. L., K. Tilly, B. Stevenson, D. Hogan, and P. Rosa. 1998. Oligopeptide permease in *Borrelia burgdorferi*: putative peptide-binding components encoded by both chromosomal and plasmid loci. *Microbiology* **144**:1033–1044.
- Bos, M. P., V. Robert, and J. Tommassen. 2007. Biogenesis of the gram-negative bacterial outer membrane. *Annu. Rev. Microbiol.* **61**:191–214.
- Brandt, M. E., B. S. Riley, J. D. Radolf, and M. V. Norgard. 1990. Immunogenic integral membrane proteins of *Borrelia burgdorferi* are lipoproteins. *Infect. Immun.* **58**:983–991.
- Braun, V., and K. Rehn. 1969. Chemical characterization, spatial distribution and function of a lipoprotein (murein-lipoprotein) of the *E. coli* cell wall. The specific effect of trypsin on the membrane structure. *Eur. J. Biochem.* **10**:426–438.
- Bunikis, J., and A. G. Barbour. 1999. Access of antibody or trypsin to an integral outer membrane protein (P66) of *Borrelia burgdorferi* is hindered by Osp lipoproteins. *Infect. Immun.* **67**:2874–2883.
- Bunikis, J., H. Mirian, E. Bunikiene, and A. G. Barbour. 2001. Non-heritable change of a spirochaete's phenotype by decoration of the cell surface with exogenous lipoproteins. *Mol. Microbiol.* **40**:387–396.
- Carroll, J. A., P. E. Stewart, P. Rosa, A. F. Elias, and C. F. Garon. 2003. An enhanced GFP reporter system to monitor gene expression in *Borrelia burgdorferi*. *Microbiology* **149**:1819–1828.
- Casjens, S., et al. 2000. A bacterial genome in flux: the twelve linear and nine circular extrachromosomal DNAs in an infectious isolate of the Lyme disease spirochete *Borrelia burgdorferi*. *Mol. Microbiol.* **35**:490–516.
- Chen, J. C., P. H. Viollier, and L. Shapiro. 2005. A membrane metalloprotease participates in the sequential degradation of a *Caulobacter* polarity determinant. *Mol. Microbiol.* **55**:1085–1103.
- Chen, S., O. S. Kumru, and W. R. Zückert. 9 September 2011. Determination of *Borrelia* surface lipoprotein anchor topology by surface proteolysis. *J. Bacteriol.* doi:10.1128/JB.05849-11.
- Cluss, R. G., D. A. Silverman, and T. R. Stafford. 2004. Extracellular secretion of the *Borrelia burgdorferi* Oms28 porin and Bgp, a glycosaminoglycan binding protein. *Infect. Immun.* **72**:6279–6286.
- Cowles, C. E., Y. Li, M. F. Semmelhack, I. M. Cristea, and T. J. Silhavy. 2011. The free and bound forms of Lpp occupy distinct subcellular locations in *Escherichia coli*. *Mol. Microbiol.* **79**:1168–1181.
- Cox, D. L., et al. 1996. Limited surface exposure of *Borrelia burgdorferi* outer surface lipoproteins. *Proc. Natl. Acad. Sci. U. S. A.* **93**:7973–7978.
- Fraser, C. M., et al. 1997. Genomic sequence of a Lyme disease spirochaete, *Borrelia burgdorferi*. *Nature* **390**:580–586.
- Gennity, J. M., and M. Inouye. 1991. The protein sequence responsible for lipoprotein membrane localization in *Escherichia coli* exhibits remarkable specificity. *J. Biol. Chem.* **266**:16458–16464.
- Gopalakrishna, R., and W. B. Anderson. 1982. Ca^{2+} -induced hydrophobic site on calmodulin: application for purification of calmodulin by phenyl-Sepharose affinity chromatography. *Biochem. Biophys. Res. Commun.* **104**:830–836.
- Guerini, D., and J. Krebs. 1983. Influence of temperature and denaturing agents on the structural stability of calmodulin. A 1H -nuclear magnetic resonance study. *FEBS Lett.* **164**:105–110.
- Hansen, R. S., and J. A. Beavo. 1982. Purification of two calcium/calmodulin-dependent forms of cyclic nucleotide phosphodiesterase by using conformation-specific monoclonal antibody chromatography. *Proc. Natl. Acad. Sci. U. S. A.* **79**:2788–2792.
- Ho, S. N., H. D. Hunt, R. M. Horton, J. K. Pullen, and L. R. Pease. 1989. Site-directed mutagenesis by overlap extension using the polymerase chain reaction. *Gene* **77**:51–59.
- Jong, W. S., et al. 2007. Limited tolerance towards folded elements during secretion of the autotransporter Hbp. *Mol. Microbiol.* **63**:1524–1536.
- Katona, L. I., G. Beck, and G. S. Habicht. 1992. Purification and immunological characterization of a major low-molecular-weight lipoprotein from *Borrelia burgdorferi*. *Infect. Immun.* **60**:4995–5003.
- Kovacs-Simon, A., R. W. Titball, and S. L. Michell. 2011. Lipoproteins of bacterial pathogens. *Infect. Immun.* **79**:548–561.
- Kretsinger, R. H., S. E. Rudnick, and L. J. Weissman. 1986. Crystal structure of calmodulin. *J. Inorg. Biochem.* **28**:289–302.
- Kudryashev, M., et al. 2009. Comparative cryo-electron tomography of pathogenic Lyme disease spirochetes. *Mol. Microbiol.* **71**:1415–1434.
- Kumru, O. S., R. J. Schulze, M. V. Rodnin, A. S. Ladokhin, and W. R. Zückert. 2011. Surface localization determinants of *Borrelia* OspC/Vsp family lipoproteins. *J. Bacteriol.* **193**:2814–2825.
- Kumru, O. S., R. J. Schulze, J. G. Slusser, and W. R. Zückert. 2010. Development and validation of a FACS-based lipoprotein localization screen in the Lyme disease spirochete *Borrelia burgdorferi*. *BMC Microbiol.* **10**:277.
- Labandeira-Rey, M., and J. T. Skare. 2001. Decreased infectivity in *Borrelia burgdorferi* strain B31 is associated with loss of linear plasmid 25 or 28-1. *Infect. Immun.* **69**:446–455.
- Lawson, C. L., B. H. Hung, A. G. Barbour, and W. R. Zückert. 2006. Crystal

- structure of neurotropism-associated variable surface protein 1 (Vsp1) of *Borrelia turicatae*. *J. Bacteriol.* **188**:4522–4530.
36. Lenhart, T. R., and D. R. Akins. 2010. *Borrelia burgdorferi* locus BB0795 encodes a BamA orthologue required for growth and efficient localization of outer membrane proteins. *Mol. Microbiol.* **75**:692–709.
 37. Lewenza, S., D. Vidal-Ingigliardi, and A. P. Pugsley. 2006. Direct visualization of red fluorescent lipoproteins indicates conservation of the membrane sorting rules in the family *Enterobacteriaceae*. *J. Bacteriol.* **188**:3516–3524.
 38. Mbow, M. L., R. D. J. Gilmore, and R. G. Titus. 1999. An OspC-specific monoclonal antibody passively protects mice from tick-transmitted infection by *Borrelia burgdorferi* B31. *Infect. Immun.* **67**:5470–5472.
 39. Nally, J. E., J. F. Timoney, and B. Stevenson. 2001. Temperature-regulated protein synthesis by *Leptospira interrogans*. *Infect. Immun.* **69**:400–404.
 40. Narita, S., and H. Tokuda. 2007. Amino acids at positions 3 and 4 determine the membrane specificity of *Pseudomonas aeruginosa* lipoproteins. *J. Biol. Chem.* **282**:13372–13378.
 41. Norris, S. J., J. Coburn, J. M. Leong, L. T. Hu, and M. Höök. 2010. Pathobiology of Lyme disease *Borrelia*, p. 299–332. In D. S. Samuels and J. D. Radolf (ed.), *Borrelia: molecular biology, host interaction, and pathogenesis*. Caister Academic Press, Norfolk, United Kingdom.
 42. Posey, J. E., and F. C. Gherardini. 2000. Lack of a role for iron in the Lyme disease pathogen. *Science* **288**:1651–1653.
 43. Promnares, K., et al. 2009. *Borrelia burgdorferi* small lipoprotein Lp6.6 is a member of multiple protein complexes in the outer membrane and facilitates pathogen transmission from ticks to mice. *Mol. Microbiol.* **74**:112–125.
 44. Purser, J. E., and S. J. Norris. 2000. Correlation between plasmid content and infectivity in *Borrelia burgdorferi*. *Proc. Natl. Acad. Sci. U. S. A.* **97**:13865–13870.
 45. Radolf, J. D., et al. 1995. Characterization of outer membranes isolated from *Borrelia burgdorferi*, the Lyme disease spirochete. *Infect. Immun.* **63**:2154–2163.
 46. Sadziene, A., D. D. Thomas, and A. G. Barbour. 1995. *Borrelia burgdorferi* mutant lacking Osp: biological and immunological characterization. *Infect. Immun.* **63**:1573–1580.
 47. Samuels, D. S. 1995. Electrotransformation of the spirochete *Borrelia burgdorferi*. *Methods Mol. Biol.* **47**:253–259.
 48. Sanyal, S., and A. K. Menon. 2009. Flipping lipids: why an' what's the reason for? *ACS Chem. Biol.* **4**:895–909.
 49. Sauer, F. G., H. Remaut, S. J. Hultgren, and G. Waksman. 2004. Fiber assembly by the chaperone-usher pathway. *Biochim. Biophys. Acta* **1694**:259–267.
 50. Schulze, R. J., S. Chen, O. S. Kumru, and W. R. Zückert. 2010. Translocation of *Borrelia burgdorferi* surface lipoprotein OspA through the outer membrane requires an unfolded conformation and can initiate at the C-terminus. *Mol. Microbiol.* **76**:1266–1278.
 51. Schulze, R. J., and W. R. Zückert. 2006. *Borrelia burgdorferi* lipoproteins are secreted to the outer surface by default. *Mol. Microbiol.* **59**:1473–1484.
 52. Seydel, A., P. Gounon, and A. P. Pugsley. 1999. Testing the '+2 rule' for lipoprotein sorting in the *Escherichia coli* cell envelope with a new genetic selection. *Mol. Microbiol.* **34**:810–821.
 53. Silva-Herzog, E., F. Ferracci, M. W. Jackson, S. S. Joseph, and G. V. Plano. 2008. Membrane localization and topology of the *Yersinia pestis* YscJ lipoprotein. *Microbiology* **154**:593–607.
 54. Skare, J. T., et al. 1995. Virulent strain associated outer membrane proteins of *Borrelia burgdorferi*. *J. Clin. Invest.* **96**:2380–2392.
 55. Sklar, J. G., T. Wu, D. Kahne, and T. J. Silhavy. 2007. Defining the roles of the periplasmic chaperones SurA, Skp, and DegP in *Escherichia coli*. *Genes Dev.* **21**:2473–2484.
 56. Stewart, P. E., R. Thalken, J. L. Bono, and P. Rosa. 2001. Isolation of a circular plasmid region sufficient for autonomous replication and transformation of infectious *Borrelia burgdorferi*. *Mol. Microbiol.* **39**:714–721.
 57. Whetstone, C. R., J. G. Slusser, and W. R. Zückert. 2009. Development of a single-plasmid-based regulatable gene expression system for *Borrelia burgdorferi*. *Appl. Environ. Microbiol.* **75**:6553–6558.
 58. Yamaguchi, K., F. Yu, and M. Inouye. 1988. A single amino acid determinant of the membrane localization of lipoproteins in *E. coli*. *Cell* **53**:423–432.
 59. Zhang, M., T. Tanaka, and M. Ikura. 1995. Calcium-induced conformational transition revealed by the solution structure of apo calmodulin. *Nat. Struct. Biol.* **2**:758–767.
 60. Zückert, W. R. 2007. Laboratory maintenance of *Borrelia burgdorferi*. *Curr. Protoc. Microbiol.* **2007**:Chapter 12, Unit 12C.1.
 61. Zückert, W. R., T. A. Kerentseva, C. L. Lawson, and A. G. Barbour. 2001. Structural conservation of neurotropism-associated VspA within the variable *Borrelia* Vsp-OspC lipoprotein family. *J. Biol. Chem.* **276**:457–463.
 62. Zückert, W. R., J. E. Lloyd, P. E. Stewart, P. A. Rosa, and A. G. Barbour. 2004. Cross-species surface display of functional spirochetal lipoproteins by recombinant *Borrelia burgdorferi*. *Infect. Immun.* **72**:1463–1469.
 63. Zückert, W. R., J. Meyer, and A. G. Barbour. 1999. Comparative analysis and immunological characterization of the *Borrelia* Bdr protein family. *Infect. Immun.* **67**:3257–3266.